Hindawi
Journal of Nanomaterials
Volume 2021, Article ID 2270472, 10 pages
https://doi.org/10.1155/2021/2270472

Research Article

Ecofriendly/Rapid Synthesis of Silver Nanoparticles Using Extract of Waste Parts of Artichoke (*Cynara scolymus* L.) and Evaluation of their Cytotoxic and Antibacterial Activities

Ayşe Baran,[1] Mehmet Fırat Baran,[2] Cumali Keskin,[2] Sevgi Irtegun Kandemir,[3] Mahbuba Valiyeva,[4] Sevil Mehraliyeva,[4] Rovshan Khalilov,[5,6,7] and Aziz Eftekhari[7,8]

[1]*Department of Biology, Graduate Education Institute, Mardin Artuklu University, Mardin, Turkey*
[2]*Medical Laboratory Techniques, Vocational Higher School of Healthcare Studies, Mardin Artuklu University, Mardin, Turkey*
[3]*Department of Medical Biology, Faculty of Medicine, Dicle University, Diyarbakir, Turkey*
[4]*Department of Pharmaceutical Technology and Management, Azerbaijan Medical University, Baku, Azerbaijan*
[5]*Department of Biophysics and Biochemistry, Baku State University, Baku, Azerbaijan*
[6]*Institute of Radiation Problems, National Academy of Sciences of Azerbaijan, Baku, Azerbaijan*
[7]*Department of Biology and Chemistry, Drohobych Ivan Franko State Pedagogical University, Drohobych, Ukraine*
[8]*Toxicology and Pharmacology Department, Maragheh University of Medical Sciences, Maragheh, Iran*

Correspondence should be addressed to Cumali Keskin; ckeskinoo@gmail.com and Aziz Eftekhari; ftekhari@ymail.com

Received 5 August 2021; Revised 18 August 2021; Accepted 1 September 2021; Published 14 September 2021

Academic Editor: Shanmugam Rajeshkumar

Recycling wastes and providing their use in useful fields attract attention every day. In our study, with the extract prepared from the parts of the *Cynara scolymus* L. (artichoke) plant that is not suitable for human consumption, silver nanoparticles were easily synthesized in an ec-friendly, energy-free way. Characterization of the obtained nanoparticles was done with a UV-visible spectrophotometer (UV-Vis.), fourier transform infrared spectroscopy (FTIR), X-ray diffraction diffractometer (XRD), scanning electron microscope (SEM), transmission electron microscopy (TEM), and zeta potential analysis data. In these data, it was determined that AgNPs have a maximum absorbance at 458.8 nm wavelength, a crystal nanosize of 28.78 nm, and a spherical appearance. The zeta potential of (-) 16.9 mV indicates that silver nanoparticles exhibit a stable structure. Particles show antimicrobial effects on pathogenic species at concentrations of 0.03-0.25 μg/ml, and it was determined by using the minimum inhibition concentration (MIC) microdilution method. By examining their cytotoxic effects on U118, CaCo-2, and Skov-3 cancer cell lines and healthy HDF cell lines by the MTT method, concentrations of inhibitive effects on survival were determined.

1. Introduction

Metallic nanoparticles are valuable materials with their widespread use. Nanoparticles such as silver (Ag), gold (Au), iron (Fe), and zinc (Zn) are some of them. There are different methods such as heat treatment and photochemical and chemical processes in obtaining them [1]. Although the application stages of these methods are difficult, they also bring high costs. Another disadvantage is that it contains toxic chemicals in the process. Against these methods, the synthesis of metallic nanoparticles with ecofriendly biological methods has recently attracted considerable attention [2].

Silver nanoparticles (AgNPs) are used in many different fields such as medical [3], bioremediation studies [4], catalysis applications [5], food [6], cosmetics industry [7], agricultural activities [8], and electronics [9]. Biological resources such as algae [10], bacteria [11], fungi [12], and plants [13] are used in the synthesis of AgNPs by biological methods. Among these, the use of plant sources, when compared to other organisms, to obtain a greater amount of

nanoparticles, the more stable particles obtained [14], the simpler and more economical application steps [15] increase the preference for this field. Plants' leaves [16], fruits [17], roots [18], flowers [19], and aboveground parts of the plant [20] are structures used for the synthesis of AgNPs.

Bioactive components such as alcohols, flavonoids, phenols, and terpenoids found in the structure of plant sources form AgNPs by reducing Ag + ions in the aqueous structure to the Ago form [21].

Cynarascolymus L. (artichoke) is a herbaceous plant cultivated in the Mediterranean region since ancient times. Today, it is widely cultured in many parts of the world. The leaf contains caffeinated quinic acid derivatives, flavonoids, lactones, tannin, and inulin. It prevents lipid peroxidation through polyphenols and flavonoids in artichoke content. It is known that this effect is caused by strong antioxidants such as cynarin and silymarin [22]. The head part is the popular vegetable consumed. It is consumed by making salads, jams, and canned food [23]. It creates a large amount of waste, except for the consumed part.

This study is aimed at synthesizing and characterizing AgNPs by using the extract obtained with the parts of the artichoke in a waste state economically and simply, with an eco-riendly method, and to examine their antimicrobial and cytotoxic activities.

2. Material and Method

2.1. Plant Material. Artichoke (*Cynarascolymus*) is a perennial herb with purple flowers belonging to the *Asteraceae* (Compositae) family. Artichoke, which is rich in antioxidants, is often grown in Mediterranean countries. As the study material, the parts of the artichoke fruit that are not consumed as food were used [23].

2.2. Instruments. The analysis was made by using, respectively, PerkinElmer one UV-visible spectrophotometer (UV-Vis.), Rad B-DMAX II computer-controlled X-ray diffractometer (XRD), EVO 40 LEQ scanning electron microscopy (SEM), and Jeol Jem. 1010 transmission electron microscopy (TEM), RadB-DMAX II computer-controlled energy dispersive X-ray diffraction (EDX), and Malvern zeta potential devices were used to determine the formation, presence, crystal structure, dimensions, morphological appearance, and surface structures of AgNPs. Besides, PerkinElmer one fourier transform infrared spectroscopy (FTIR) device was used to evaluate the bioactive groups in the extract participating in reduction. The OHAUS FC 5706 model refrigerated centrifuge (6000 rpm) was used to separate the AgNPs from the extract at the end of synthesis.

Sigma-Aldrich brand solid compound form of % 98.8 $AgNO_3$ (silver nitrate) was used. Commercially purchased vancomycin, colistin, and fluconazole were used as standard antibiotics.

2.3. Plant Extract and Solution Preparation. The edible part of the 3 kg artichoke fruit is approximately 500 g. The rest is in the waste state as it is not consumed. After weighing 200 g of the parts to be discarded, they were cut into small pieces and dried under room conditions for use as material. It undergoes a series of washing processes to purify it from material residues. The extraction process was carried out at room temperature using a heated magnetic stirrer (150 rpm). In the extraction process, after the mixture reaches boiling temperature, it is left to boil for 5 minutes. Then, it was cooled at room temperatureand then the extract and residue are separated using Whatman no. 1 filter paper. The obtained extract was made ready to use for synthesis.

A solution with a concentration of 20 mM (millimolar) was prepared from the $AgNO_3$ salt.

2.4. Synthesis of AgNPs and Characterization. 500 ml of plant extract and 20 mM $AgNO_3$ solution was transferred into a 2000 ml glass flask. It was left on a stable surface at room conditions after simple mixing. Observations were made depending on the time. Samples were taken according to the color change, wavelength, and absorbance measurements were made in the UV-vis spectrophotometer.

To detect the formation and presence of AgNP analyses, the UV-visible spectrophotometer was used. Functional groups of bioactive components involved in reduction were evaluated with FTIR analysis data. A high-speed centrifuge was used to separate the AgNPs from the liquid phase after synthesis. After the reaction was finished, the dark solution was centrifuged at 6000 rpm for 25 minutes. The centrifuge process was repeated several times by adding distilled water. Then, the removed particles from the residue were left to dry at 80°C.The dried and powdered material was used in FTIR analysis. XRD analysis results were examined to determine the crystal sizes and structures. SEM, TEM, and EDX data were evaluated to determine the morphological structure and element composition content. The zeta potential analysis results were examined in the surface analysis of nanoparticles and in determining the charge distribution.

2.5. Determination of Antimicrobial Activity Using the Minimum Inhibition Concentration (MIC) Microdilution Method. Staphylococcus aureus (S.aureus) ATCC 25923, Escherichia coli (E. coli) ATCC25922 strains, and *Candida albicans (C.albicans)*clinic isolate were obtained from İnönü University Medical Faculty Hospital Microbiology Laboratory, and *Bacillus subtilis (B. subtilis) ATCC 11774* and *Pseudomonas aeruginosa* (*P. aeruginosa*) *ATCC27853* were obtained from Artuklu University Microbiology Research Laboratory.

Gram-positive (*S. aureus* and *B. subtilis*) and Gram-negative (*P. aeruginosa* and *E. coli*) bacteria were inoculated on a nutrient agar medium. *C. Albicans* yeast was inoculated on sabouraud dextrose agar medium and left to grow in an oven at 37°C overnight. Following the growth control the next day, microorganism suspensions were prepared according to McFarland standard 0.5 [24] (the colony in 1.5×10^8 units (CFU) ml^{-1}) concentration for each of the microorganisms grown from the plates in solid form.

Muller Hinton broth (for bacteria), RPMI (Roswell Park Memorial Institute) broth for yeast, and AgNP solution prepared at concentrations of 20 $\mu g/ml^{-1}$ were added to 96 well microplates. A series of dilutions were made to the first well

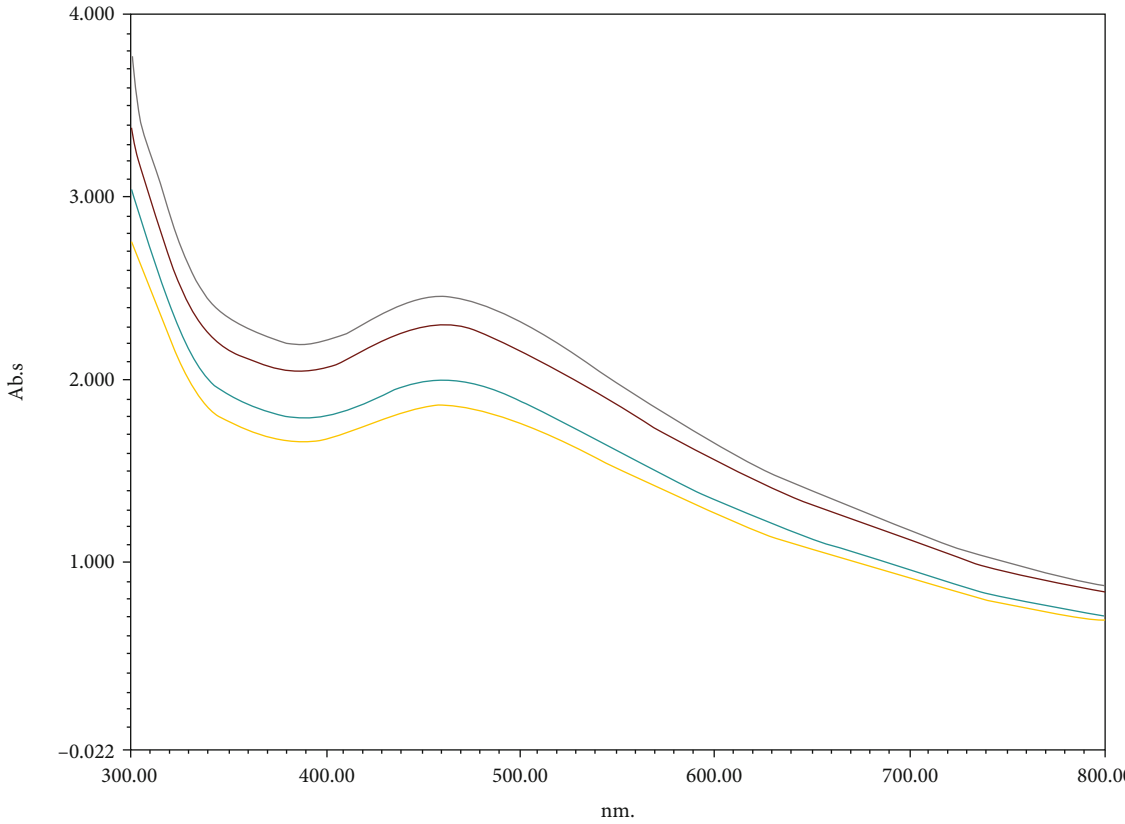

Figure 1: UV-vis showing the formation and presence of AgNPs: spectrophotometer data.

and then the other wells. Then, suspension prepared for each microorganism was added to each diluted well.

To compare the effects of AgNPs, the same application steps were repeated using vancomycin for Gram-positive strains, colistin for Gram-negative, and finally fluconazole antibiotics for the yeast *C. albicans*. Microplates were allowed to grow at 37°C for 24 hours. At the end of the period, the concentration of the well before the well where the growth started was determined as the minimum inhibition concentration.

2.6. Analyzing of Cytotoxic Effects of AgNPs. Cytotoxic effect application was made in Dicle University Scientific Research Centre Cell Culture Laboratory with human dermal fibroblast (HDF), glioblastoma (U118), human colorectal adenocarcinoma (CaCo-2), and ovarian sarcoma (Skov-3) cells obtained from the American Type Culture Collection (ATCC).

The 3 cell types used were cultured in Dulbecco's Modified Eagle's Medium (DMEM) 75 t-flasks that include 10% FBS, 100 U/ml penicillin-streptomycin (Penstrep.), and 2 mM L-glutamine.Over sarcoma (Skov-3) cells were cultured in Roswell Park Memorial Institute (RPMI) 75 t-flasks that include %10 FBS and 100 U/ml penstrep.

The cultured flasks were incubated at 37°C, 5% CO_2, 95% air, and humidity conditions. After the cells reached approximately 80% confluence in the hemocytometermeasurement, they were suspended in different concentrations, transferred to 96 well microplates, and subjected to an overnight incubation. The next day, cells were treated with nanoparticles with concentrations of 200 μg/ml, 100 μg/ml, 50 μg/ml, and 25 μg/ml and incubated for 48 hours. After waiting, MTT solution was added to the plate wells, 3 hours of incubation, and then DMSO was added and left at room temperature for 15 minutes. The absorbance of the microplates at 540 nm wavelength was measured using the Multi ScanGo, Thermo instrument.

Using these absorbance values, the concentration in which the percentage of viability of AgNPs is inhibited on cells was calculated: %viability = U/C × 100 [25, 26].

U defines absorbances of cells treated with AgNPs, and C defines the absorbance values of control cells.

3. Result and Discussion

3.1. UV-vis. Spectrophotometer Data. Colour transformation from yellow to dark brown was observed one hour after mixing the plant extract and 20 mM $AgNO_3$ solution [2]. This color change is caused by the reduction of Ag+ ions to Ago while transforming to AgNPs and the occurrence of vibrations (SPR) on the plasma surface [27, 28]. On the UV vis. device readings of samples taken regarding color changes, maximum absorbance value was found at 458.8 nm wavelength (Figure 1). It refers to the samples taken every two minutes in the UV-Vis spectrophotometer.

These peaks represent the maximum absorption of samples taken at different times.

The results of color change and maximum absorbance wavelength are the data showing the formation and presence of AgNPs in the dark-colored liquid [24, 29].

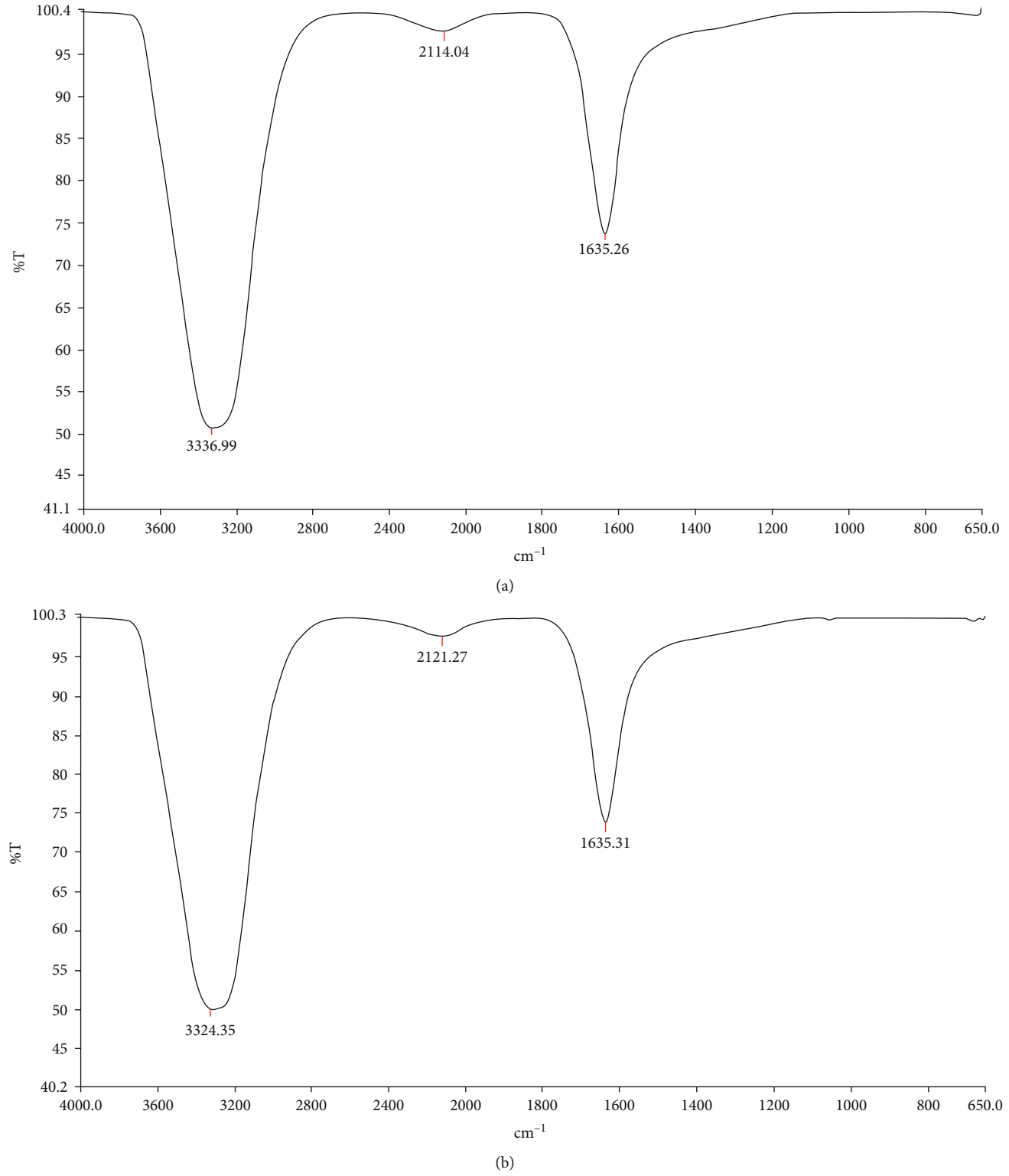

Figure 2: Infrared spectra of (a) extract of *Cynara scolymus* L. and (b) the reducing functional groups that play a role in the formation of AgNPs.

In synthesis studies using plant extracts, the maximum absorbance wavelength results of 460 nm [30] and 453 nm [9] have been associated with the presence of AgNPs.

3.2. FTIR Analysis Data. The functional groups involved in reduction were evaluated by looking at the FTIR results. Frequency shifts occurred at 3336.99-3324.35 cm^{-1}, 1635.26-

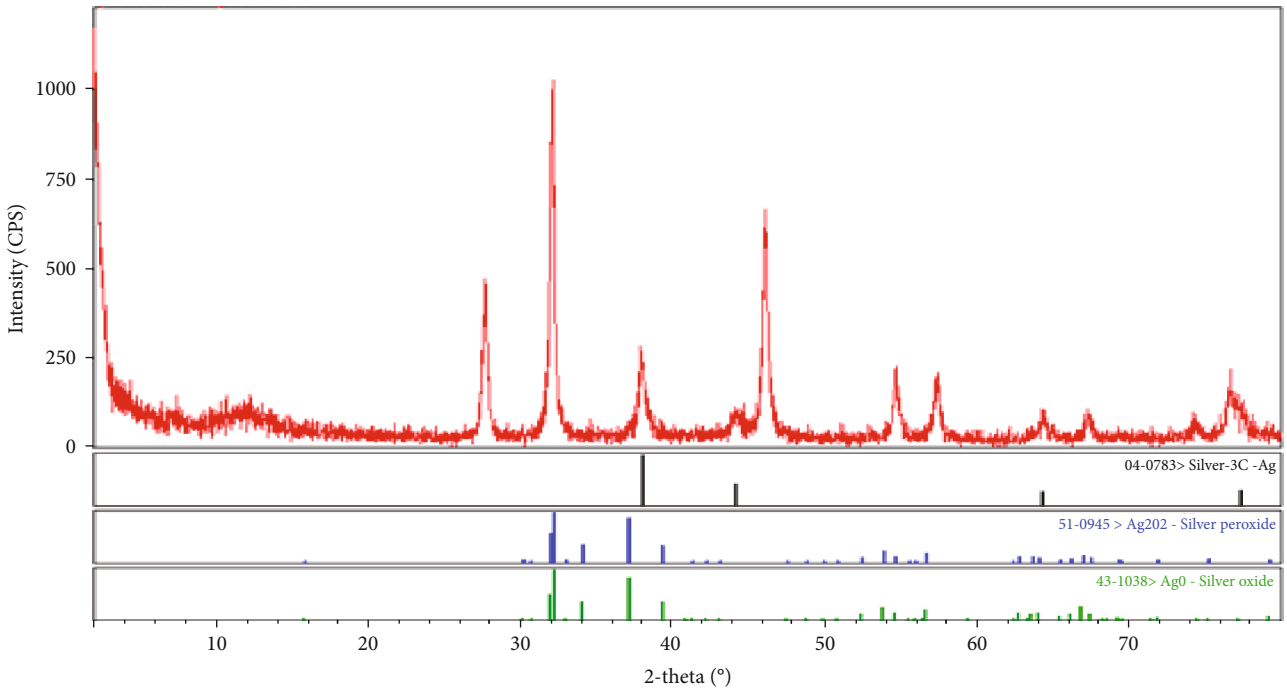

Figure 3: X-ray diffraction data of the crystal pattern of AgNPs.

1635.31 cm^{-1}, and 2114.04-2121.27 cm^{-1}. The shifts in these frequencies suggest that -OH (hydroxyl) groups [15], N-H amine groups [31], and C≡C alkyne groups [32] are functional groups involved in the reduction (Figure 2).

3.3. XRD Analysis Data. At 2θ, in the XRD results, it was seen that the crystal structure of silver was cubic, and the peaks belong to 111°, 200°, 220°, and 311° [33]. The values of these peaks were read as 32.16, 46.10, 64.44, and 76.68, respectively (Figure 3).

Using the peak values, the crystal nanosize was calculated according to the Debye-Scherrer equation ($D = K\lambda/(\beta \cos \theta)$ [33].

The meanings of the symbols in this equation are D is the particle size, K is the constant value (0.90), X-ray wavelength λ value (1.5418 Å), β value of peak at maximum height (FWHM), and Bragg θ angle of a high peak. As a result of the calculation, it was concluded that it has a crystal nanosize of 28.78 nm. In other studies calculating the crystal nanosize of AgNPs using the Debye-Scherrer equation, 35 nm [18] and 40 nm [34] crystal nanosizes were calculated.

3.4. SEM, TEM, and EDX Analysis Data. SEM, TEM, and EDX analysis data were used to determine the morphological structures and element compositions of AgNPs obtained after synthesis (Figure 4). It was determined that obtained AgNPs are in spherical view [34, 35]. Strong peaks of silver in EDX data indicate that the element composition is largely silver content and the presence of AgNPs [36]. Weak C and O peaks are due to contamination from extract [37] (Figure 4).

3.5. Zeta Potential of AgNPs. In the zeta potential analyses made to determine the surface charges of AgNPs, it was examined whether AgNPs were negatively or positively charged. As seen in Figure 5, the zeta potentials of AgNPs obtained were measured as -16.9 mV. When AgNPs are in positive and negative charges, they show clustering and clumping features [26]. The (-)16.9 mV value we obtained shows that AgNPs have only negative charges and exhibit a stable structure. Since the silver nanoparticles we synthesize are of plant origin, it is natural to have a negative zeta potential. We think that this is due to the negatively charged structures in the plant structure. Having only a negative charge indicates that there is no clustering and clumping [38]. These negative charges may be due to the extract. The zeta potentials of AgNPs were found to be -14 mV [25] and -19 mV [26] in the studies. In a synthesis study, a zeta potential value of +5.68 mV was found, and it was reported that AgNPs exhibit clustering and clumping character [2].

3.6. Evaluation of Antimicrobial Activities of AgNPs. When we evaluated the activities of AgNPs, we obtained on pathogen species, and we determined that concentrations of 0.12 and 0.25 μg/ml and were effective on Gram-positive *S. aureus* and *B.subtilis* bacteria, respectively. We determined that the concentration of 0.07 and 0.13 μg/ml was effective on *P. aeruginosa* and *E. coli* in Gram-negative bacteria, respectively. The lowest concentration where AgNPs are effective is the concentration of 0.03 μg/ml on C. albicans yeast. When we compared the effects of AgNPs obtained with silver nitrate solution and antibiotics, we concluded that they were effective at lower concentrations against these groups (Figure 6 and Table 1).

Silver ions ionize in an aqueous structure and show a high level of reactivity. Positive silver ions interact with the negatively charged cell membranes of microorganisms with an electrostatic attraction force. After this interaction, they

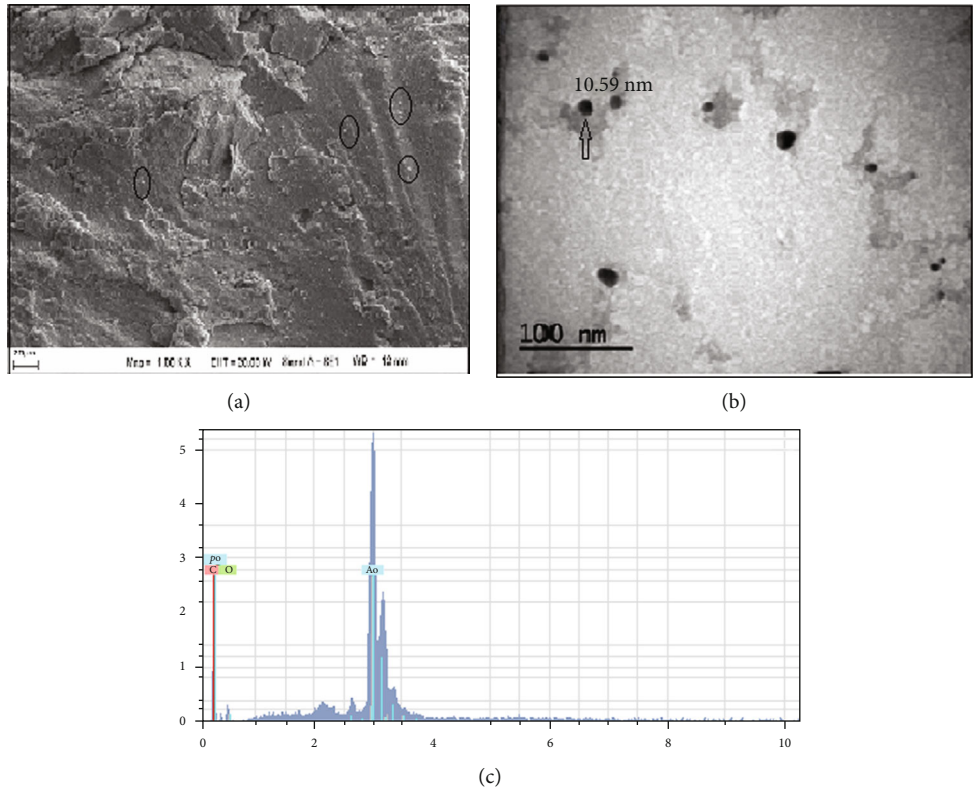

Figure 4: Morphological images and element composition of AgNPs: (a) SEM, (b) TEM images, and (c) EDX profile element.

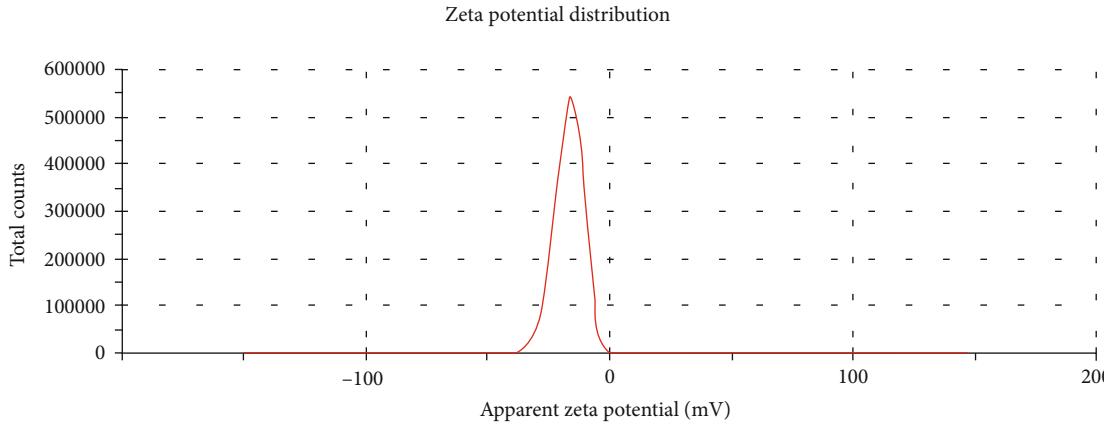

Figure 5: The zeta potential data of the surface charge distributions of AgNPs.

cause an increase in reactive oxygen species (ROS). With the increase of ROS, the cell wall structure is disrupted. The functions of the cell membrane and the nucleus membrane are impaired and undergo structural changes. The functions of structures such as DNA, RNA, and protein synthesis that have an affinity for these species are disrupted. Cell death occurs with cellular destruction [39–42].

When we examined some researches on the antimicrobial effects of AgNPs, it was found that the AgNPs are obtained using the plant extract of *Pistacia vera L.*, and it was observed to be effective on *S. aureus*, *E. coli,* and *C. albicans* species at concentrations of 0.04, 0.66, and 0.16 μg/ml, respectively [15]. In a study aimed at obtaining AgNPs in different sizes, it was determined that those with 5 nm sizes were effective on *B. subtilis, S. aureus,* and *E. coli* with concentrations of 0.8-6 μg/ml [43]. In another study, it was emphasized that AgNPs were effective at 30 μg/ml concentration on *P.aeruginosa* [24].

AgNPs may show different effects in different strains. Among the factors that affect their activities, characteristics such as concentration, size, shape, microorganism wall structure, temperature, and pH play a decisive role [42, 44].

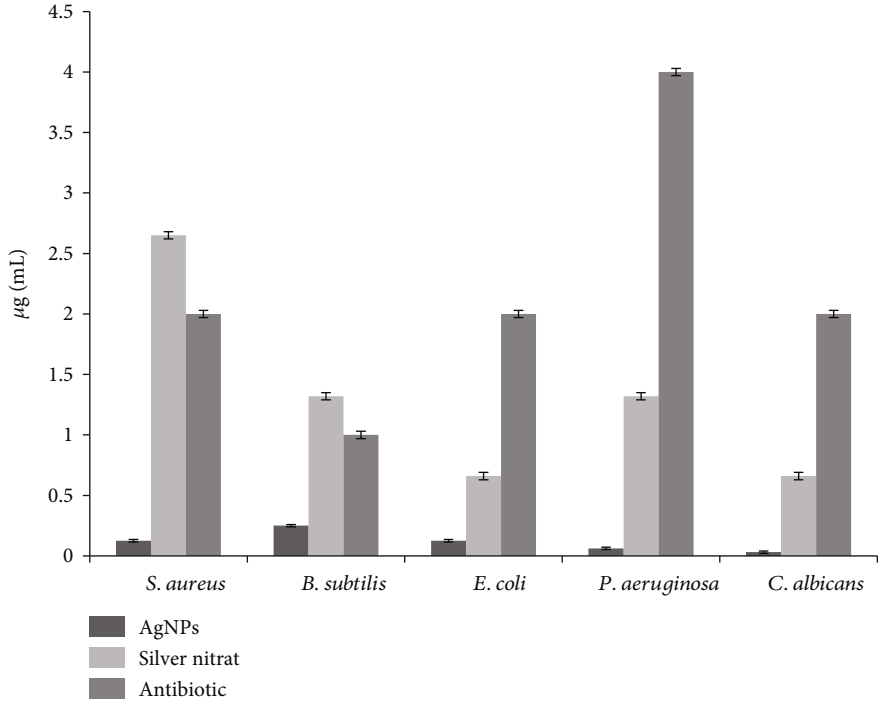

Figure 6: MIC values of AgNPs, silver nitrate solution, and antibiotics on the growth of pathogenic microorganisms.

Table 1: MIC values where AgNPs, silver nitrate, and antibiotics are effective in antimicrobial activity.

Tested organism	AgNPs μg/ml	Silver nitrate μg/ml	Antibiotic μg/ml
S. aureus ATCC 29213	0.12	2.65	2
B. subtilis ATCC 11773	0.25	1.32	1
E. coli ATCC25922	0.13	0.66	2
P. aeruginosa ATCC27833	0.07	1.32	4
C. albicans	0.03	0.66	2

3.7. Cytotoxic Activities of AgNPs. The data on the cytotoxic activities of the AgNPs we obtained on U118, HDF, CaCo-2, and Skov-3 cell lines are presented in Figure 7 and Table 2. 44.76% viability was seen on HDF cells at a concentration of 25 μg/ml. On the U118 and Skov-3 cell lines, 58.98% and 74.55% viability was determined at a concentration of 25 μg/ml, respectively. A concentration of 25 μg/ml was toxic in the U118 and CaCo-2 cell lines. The increase in the percentage of viability versus the concentration of AgNPs in the U118 cell line is due to the proliferative properties of cancer cells [45].

AgNPs exhibit strong oxidative properties. The release of the Ag + form may induce immunological, cytotoxic, and genotoxic responses in biological environments; therefore, it is of great importance to examine its effects[46]. AgNPs settle at different points in the cells. These spots are the cell membrane, nucleus, and mitochondria. AgNPs show toxic effects by inducing apoptosis with ROS increase [45, 47].

In cell line studies on the cytotoxicity of AgNPs, it was determined that CaCo-2 cells at 3.75 μg/ml [46] and Skov-3 cells at 9.4 μg/ml [25] had toxic effects. In a study conducted on HDF cell lines, it was stated that a concentration of 100 μg/ml has a toxic effect [48].

Several parameters can have a significant effect on the toxicity of nanomaterials. Some of them are concentration, exposure time, charge, the chemistry of surface composition, degree of deposition, shape, and size [41].

The different cytotoxic concentrations of AgNPs we obtained in all these studies and ourselves maybe since AgNPs are synthesized from different sources and have different sizes and morphological structures.

4. Conclusion

Artichoke (*Cynara scolymus* L.) is a plant that cannot be used except for the edible part and generates a large amount of agricultural waste. We synthesized AgNPs with an easy, economical, and ecofriendly method with the extract we prepared from these parts to transform these wastes into useful fields for human life. We characterized the AgNPs obtained with UV-vis., FTIR, SEM, TEM, EDX, XRD, and zeta potential analysis data. According to the results of the XRD analysis, the average nanosize was calculated to be 28.78 nm. As can be seen from the SEM images, it was determined that the silver nanoparticles were spherical, and the AgNPs averaged 10.59 in the TEM analysis. It was determined that AgNPs showed antimicrobial effects at low concentrations such as 0.03-0.25 μg/ml. It is important to examine and determine the toxic effects of AgNPs for their use as anticancer and antimicrobial agents in medicine. Cytotoxic effects of AgNPs on U118, HDF, CaCo-2, and Skov-3 cell lines were

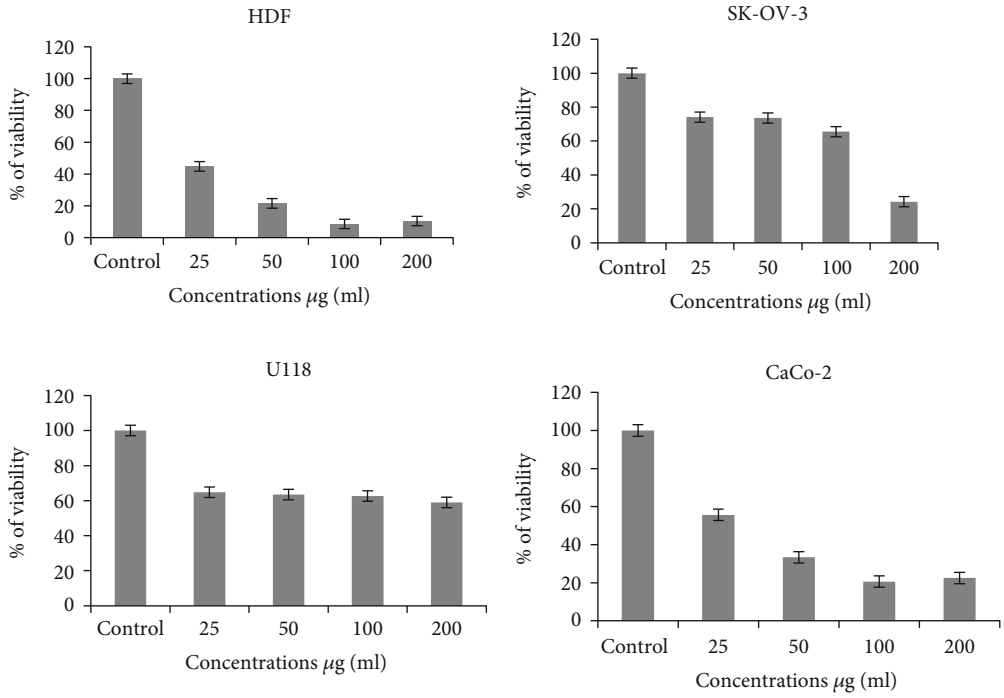

Figure 7: Viability rates of HDF, U118, CaCo-2, and Skov-3 cell lines 48 hours after interaction with AgNPs.

Table 2: Viability-suppressing concentrations of AgNPs on HDF, U118, CaCo-2, and Skov-3 cell lines.

Cell lines	25 μg/ml	50 μg/ml	100 μg/ml	200 μg/ml
HDF	44.76	21.52	8.61	10.44
U118	58.98	62.65	63.52	64.70
CaCo-2	55.64	33.37	20.624	22.50
Skov-3	74.15	73.62	65.57	24.25

examined. We determined an approximately 50% inhibition on cancer cell lines at a concentration of 25 μg/ml. These rates can be increased by developing method steps. It can be qualified to supply the demand for antimicrobial and anticancer agents.

Data Availability

All data used to support the findings of this study are included within the article.

Conflicts of Interest

The authors declare that there are no conflicts of interest regarding the publication of this paper.

Acknowledgments

The authors are thankful to Mardin Artuklu University for providing all necessary research facilities to carry out this research.

References

[1] F. Mohammadi, M. Yousefi, and R. Ghahremanzadeh, "Green synthesis, characterization and antimicrobial activity of silver nanoparticles (AgNps) using leaves and stems extract of some plants," *Advanced Journal of Chemistry-Section A*, vol. 2, no. 4, pp. 266–275, 2019.

[2] Z. A. Ali, R. Yahya, S. D. Sekaran, and R. Puteh, "Green synthesis of silver nanoparticles using apple extract and its antibacterial properties," *Advances in Materials Science and Engineering*, vol. 2016, Article ID 4102196, 6 pages, 2016.

[3] J. Y. Song and B. S. Kim, "Rapid biological synthesis of silver nanoparticles using plant leaf extracts," *Bioprocess and Biosystems Engineering*, vol. 32, no. 1, pp. 79–84, 2009.

[4] B. Thomas, B. S. M. Vithiya, T. A. A. Prasad et al., "Antioxidant and photocatalytic activity of aqueous leaf extract mediated green synthesis of silver nanoparticles UsingPassiflora edulis f. flavicarpa," *Journal of Nanoscience and Nanotechnology*, vol. 19, no. 5, pp. 2640–2648, 2019.

[5] P. Rani, V. Kumar, P. P. Singh et al., "Highly stable AgNPs prepared via a novel green approach for catalytic and photocatalytic removal of biological and non-biological pollutants," *Environment International*, vol. 143, 2020.

[6] J. A. Gudadhe, A. Yadav, A. Gade, P. D. Marcato, N. Durán, and M. Rai, "Preparation of an agar-silver nanoparticles (A-AgNp) film for increasing the shelf-life of fruits," *IET Nanobiotechnology*, vol. 8, no. 4, pp. 190–195, 2014.

[7] A. C. P. Dias, G. Marslin, Selvakesavan, F. Gregory, and B. Sarmento, "Antimicrobial activity of cream incorporated with silver nanoparticles biosynthesized from Withania somnifera," *International Journal of Nanomedicine*, vol. 10, pp. 5955–5963, 2015.

[8] S. D. Gupta, A. Agarwal, and S. Pradhan, "Phytostimulatory effect of silver nanoparticles (AgNPs) on rice seedling growth:

an insight from antioxidative enzyme activities and gene expression patterns," *Ecotoxicology and Environmental Safety*, vol. 161, pp. 624–633, 2018.

[9] S. Sampaio and J. C. Viana, "Production of silver nanoparticles by green synthesis using artichoke (Cynara scolymusL.) aqueous extract and measurement of their electrical conductivity," *Advances in Natural Sciences: Nanoscience and Nanotechnology*, vol. 9, no. 4, pp. 1–10, 2018.

[10] S. N. Sinha, D. Paul, N. Halder, D. Sengupta, and S. K. Patra, "Green synthesis of silver nanoparticles using fresh water green alga Pithophora oedogonia (Mont.) Wittrock and evaluation of their antibacterial activity," *Applied Nanoscience*, vol. 5, no. 6, pp. 703–709, 2015.

[11] K. Gopalu, J. Matheswaran, G. Alexander, A. L. T. Juan, K. Evgeny, and K. Denis, "Rapid biosynthesis of AgNPs using soil bacterium Azotobacter vinelandii with promising antioxidant and antibacterial activities for biomedical applications," *Journal of the Minerals, Metals and Materials Society*, vol. 69, pp. 1206–1212, 2017.

[12] G. Li, D. He, Y. Qian et al., "Fungus-mediated green synthesis of silver nanoparticles using aspergillus terreus," *International Journal of Molecular Sciences*, vol. 13, no. 1, pp. 466–476, 2012.

[13] C. Luna, V. H. G. Chávez, E. D. Barriga-Castro, N. O. Núñez, and R. Mendoza-Reséndez, "Biosynthesis of silver fine particles and particles decorated with nanoparticles using the extract of *Illicium verum* (star anise) seeds," *Spectrochimica Acta Part A: Molecular and Biomolecular Spectroscopy*, vol. 141, pp. 43–50, 2015.

[14] O. A. Ojo, B. E. Oyinloye, A. B. Ojo et al., "Green synthesis of silver nanoparticles (AgNPs) using Talinum triangulare (Jacq.) Willd. leaf extract and monitoring their antimicrobial activity," *Journal of Bionanoscience*, vol. 11, pp. 292–296, 2017.

[15] M. F. Baran, "Synthesıs, Characterızatıon And Investıgatıon Of Antımıcrobıal Actıvıty Of Sılver Nanopartıcles From Cydonıa oblonga Leaf.," *Applied Ecology and Environmental Research*, vol. 17, no. 2, pp. 2583–2592, 2019.

[16] S. Francis, S. Joseph, E. P. Koshy, and B. Mathew, "Green synthesis and characterization of gold and silver nanoparticles using Mussaenda glabrata leaf extract and their environmental applications to dye degradation," *Environmental Science and Pollution Research*, vol. 24, no. 21, pp. 17347–17357, 2017.

[17] B. Kumar, K. Smita, L. Cumbal, and A. Debut, "Green synthesis of silver nanoparticles using Andean blackberry fruit extract," *Saudi Journal of Biological Sciences*, vol. 24, no. 1, pp. 45–50, 2015.

[18] C. Sudhakar, K. Selvam, M. Govarthanan et al., "*Acorus calamus* rhizome extract mediated biosynthesis of silver nanoparticles and their bactericidal activity against human pathogens," *Journal, Genetic Engineering & Biotechnology*, vol. 13, no. 2, pp. 93–99, 2015.

[19] G. Karunakaran, M. Jagathambal, M. Venkatesh et al., "*Hydrangea paniculata* flower extract-mediated green synthesis of MgNPs and AgNPs for health care applications," *Powder Technology*, vol. 305, pp. 488–494, 2017.

[20] M. F. Baran, "Synthesis and antimicrobial applications of silver nanoparticles from artemisia absinthium plant," *Biological and Chemical Research*, vol. 6, pp. 96–103, 2019.

[21] S. K. Srikar, D. D. Giri, D. B. Pal, P. K. Mishra, and S. N. Upadhyay, "Green synthesis of silver nanoparticles : a review," *Green and Sustainable Chemistry*, vol. 6, no. 1, pp. 34–56, 2016.

[22] A. Mandegary, A. Saeedi, A. Eftekhari, V. Montazeri, and E. Sharif, "Hepatoprotective effect of silyamarin in individuals chronically exposed to hydrogen sulfide; modulating influence of TNF-α cytokine genetic polymorphism," *DARU Journal of Pharmaceutical Sciences*, vol. 21, no. 1, 2019.

[23] B. Biswas, K. Rogers, F. McLaughlin, D. Daniels, and A. Yadav, "Antimicrobial Activities of Leaf Extracts of Guava (Psidium guajava L.) on Two Gram-Negative and Gram-Positive Bacteria," *International Journal of Microbiology*, vol. 2013, Article ID 746165, 7 pages, 2013.

[24] W. R. Rolim, M. T. Pelegrino, B. de Araújo Lima et al., "Green tea extract mediated biogenic synthesis of silver nanoparticles: characterization, cytotoxicity evaluation and antibacterial activity," *Applied Surface Science*, vol. 463, pp. 66–74, 2019.

[25] C. D. Fahrenholtz, J. Swanner, M. Ramirez-Perez, and R. N. Singh, "Heterogeneous responses of ovarian cancer cells to silver nanoparticles as a single agent and in combination with cisplatin," *Journal of Nanomaterials*, vol. 2017, Article ID 5107485, 11 pages, 2017.

[26] I. Al-Ogaidi, M. I. Salman, F. I. Mohammad et al., "Antibacterial and cytotoxicity of silver nanoparticles synthesized in green and black tea," *World*, vol. 5, no. 1, pp. 39–45, 2017.

[27] M. J. Ahmed, G. Murtaza, F. Rashid, and J. Iqbal, "Eco-friendly green synthesis of silver nanoparticles and their potential applications as antioxidant and anticancer agents," *Drug Development and Industrial Pharmacy*, vol. 45, no. 10, pp. 1682–1694, 2019.

[28] M. F. Baran, "Green synthesıs of sılver nanopartıcles (AGNPs) usıng Pıstacıa Terebınthus leaf extract: antımıcrobıal effect and characterızatıon," *International Journal of Mathematics and Mathematical Sciences*, vol. 5, no. 2, 2018.

[29] W. Zhang and W. Jiang, "Antioxidant and antibacterial chitosan film with tea polyphenols- mediated green synthesis silver nanoparticle via a novel one-pot method," *International Journal of Biological Macromolecules*, vol. 155, pp. 1252–1261, 2020.

[30] A. D. Dwivedi and K. Gopal, "Biosynthesis of silver and gold nanoparticles using *Chenopodium album* leaf extract," *Colloids and Surfaces A: Physicochemical and Engineering Aspects*, vol. 369, no. 1–3, pp. 27–33, 2010.

[31] G. Das, H. Shin, A. Kumar, C. N. Vishnuprasad, and J. K. Patra, "Photo-mediated optimized synthesis of silver nanoparticles using the extracts of outer shell fibre of *Cocos nucifera* L. fruit and detection of its antioxidant, cytotoxicity and antibacterial potential," *Saudi Journal of Biological Sciences*, vol. 28, no. 1, pp. 980–987, 2021.

[32] M. M. Alkhulaifi, J. H. Alshehri, M. A. Alwehaibi et al., "Green synthesis of silver nanoparticles using Citrus Limon peels and evaluation of their antibacterial and cytotoxic properties," *Saudi Journal of Biological Sciences*, vol. 27, no. 12, pp. 3434–3441, 2020.

[33] A. Eren and M. F. Baran, "Green Synthesis, Characterization and Antimicrobial Activity of Silver Nanoparticles (AgNPs) from Maize (*ZEA mays* L.)," *Applied Ecology and Environmental Research*, vol. 17, no. 2, pp. 4097–4105, 2019.

[34] K. R, G. G, J. A, and G. M, "Rapid green synthesis of silver nanoparticles (AgNPs) using (Prunus persica) plants extract: exploring its antimicrobial and catalytic activities," *Journal of Nanomedicine & Nanotechnology*, vol. 8, no. 4, pp. 1–8, 2017.

[35] J. Wongpreecha, D. Polpanich, T. Suteewong, C. Kaewsaneha, and P. Tangboriboonrat, "One-pot, large-scale green synthesis of silver nanoparticles-chitosan with enhanced antibacterial

activity and low cytotoxicity," *Carbohydrate Polymers*, vol. 199, pp. 641–648, 2018.

[36] V. Kumar, R. K. Gundampati, D. K. Singh, D. Bano, M. V. Jagannadham, and S. H. Hasan, "Photoinduced green synthesis of silver nanoparticles with highly effective antibacterial and hydrogen peroxide sensing properties," *Journal of Photochemistry and Photobiology B: Biology*, vol. 162, pp. 374–385, 2016.

[37] D. Arumai Selvan, D. Mahendiran, R. Senthil Kumar, and A. Kalilur Rahiman, "Garlic, green tea and turmeric extracts-mediated green synthesis of silver nanoparticles: Phytochemical, antioxidant and *in vitro* cytotoxicity studies," *Journal of Photochemistry and Photobiology B: Biology*, vol. 180, pp. 243–252, 2018.

[38] M. P. Patil, R. D. Singh, P. B. Koli et al., "Antibacterial potential of silver nanoparticles synthesized using *Madhuca longifolia* flower extract as a green resource," *Microbial Pathogenesis*, vol. 121, pp. 184–189, 2018.

[39] V. Gopinath, S. Priyadarshini, M. F. Loke et al., "Biogenic synthesis, characterization of antibacterial silver nanoparticles and its cell cytotoxicity," *Arabian Journal of Chemistry*, vol. 10, no. 8, pp. 1107–1117, 2017.

[40] P. Singh, A. Garg, S. Pandit, V. R. S. S. Mokkapati, and I. Mijakovic, "Antimicrobial effects of biogenic nanoparticles," *Nanomaterials*, vol. 8, no. 12, pp. 1009–1019, 2018.

[41] M. K. Swamy, M. S. Akhtar, S. K. Mohanty, and U. R. Sinniah, "Synthesis and characterization of silver nanoparticles using fruit extract of *Momordica cymbalaria* and assessment of their *in vitro* antimicrobial, antioxidant and cytotoxicity activities," *Spectrochimica Acta Part A: Molecular and Biomolecular Spectroscopy*, vol. 151, pp. 939–944, 2015.

[42] N. Durán, M. Durán, M. B. JesusDe, A. B. Seabra, W. J. Fávaro, and G. Nakazato, "Silver nanoparticles: a new view on mechanistic aspects on antimicrobial activity," *Nanomedicine: Nanotechnology, Biology and Medicine*, vol. 12, no. 3, pp. 789–799, 2016.

[43] J. Li, K. Rong, H. Zhao, F. Li, Z. Lu, and R. Chen, "Highly selective antibacterial activities of silver nanoparticles against Bacillus subtilis," *Journal of Nanoscience and Nanotechnology*, vol. 13, no. 10, pp. 6806–6813, 2013.

[44] S. Rajeshkumar and L. V. Bharath, "Mechanism of plant-mediated synthesis of silver nanoparticles – a review on biomolecules involved, characterisation and antibacterial activity," *Chemico-Biological Interactions*, vol. 273, pp. 219–227, 2017.

[45] M. Morais, A. L. Teixeira, F. Dias, V. Machado, R. Medeiros, and J. A. V. Prior, "Cytotoxic effect of silver nanoparticles synthesized by green methods in cancer," *Journal of Medicinal Chemistry*, vol. 63, no. 23, pp. 14308–14335, 2020.

[46] A. Mohmed, S. Hassan, A. Fouda, M. Elgamal, and S. Salem, "Extracellular biosynthesis of silver nanoparticles using aspergillus sp. and evaluation of their antibacterial and cytotoxicity," *Journal of Applied Life Sciences International*, vol. 11, no. 2, pp. 1–12, 2017.

[47] A. R. Gliga, S. Skoglund, I. Odnevall Wallinder, B. Fadeel, and H. L. Karlsson, "Size-dependent cytotoxicity of silver nanoparticles in human lung cells: the role of cellular uptake, agglomeration and Ag release," *Particle and Fibre Toxicology*, vol. 11, no. 1, pp. 1–17, 2014.

[48] Y. Zhang, D. Yang, Y. Kong, X. Wang, O. Pandoli, and G. Gao, "Synergetic antibacterial effects of silver nanoparticles@aloe vera prepared via a green method," *Nano Biomedicine and Engineering*, vol. 2, no. 4, pp. 252–257, 2010.